

# Glioblastoma Factors Increase the Migration of Human Brain Endothelial Cells *In Vitro* by Increasing MMP-9/CXCR4 Levels

LUCIANE VIEIRA DE OLIVEIRA ROSARIO<sup>1</sup>, BARBARA GOMES DA ROSA<sup>2</sup>, THAYNAN LOPES GONCALVES<sup>1</sup>,  
DIANA ISABEL LOURENCO MATIAS<sup>3</sup>, CATARINA FREITAS<sup>2</sup> and VALERIA PEREIRA FERRER<sup>4</sup>

<sup>1</sup>*Brain's Biomedicine Lab, Paulo Niemeyer State Brain Institute, Rio de Janeiro, Brazil;*

<sup>2</sup>*Cellular Morphogenesis Lab, Biomedical Sciences Institute,  
Federal University of Rio de Janeiro, Rio de Janeiro, Brazil;*

<sup>3</sup>*Battaglia's Lab, Department of Chemistry, Christopher Ingold Building, University College London, London, U.K.;*

<sup>4</sup>*Department of Cellular and Molecular Biology, Institute of Biology,  
Fluminense Federal University, Niteroi, Brazil*

**Abstract.** *Background/Aim:* Glioblastoma (GB) is the most aggressive type of tumor in the central nervous system and is characterized by resistance to therapy and abundant vasculature. Tumor vessels contribute to the growth of GB, and the tumor microenvironment is thought to influence tumor vessels. We evaluated the molecular communication between human GB cells and human brain microvascular endothelial cells (HBMEC) *in vitro*. *Materials and Methods:* We investigated whether GB-conditioned media (GB-CM) influenced HBMEC proliferation and migration, as well as the levels of MMP-9, CXCL12, CXCR4, CXCR7, VEGFs, VEGFR-2, and WNT5a in HBMEC. *Results:* Although HBMEC proliferation was not modified, increased HBMEC migration was detected after GB-CM treatment. Furthermore, treatment of HBMEC with GB-CM resulted in increased levels of MMP-9 and CXCR4. The levels of WNT5a, VEGFs and VEGFR-2 were not affected. *Conclusion:* GB-secreted factors lead to increased endothelial cell migration and to increased levels of MMP-9 and CXCR4.

Glioblastoma (GB) is the most common and deadly type of primary brain tumor in adults (1). The hallmarks of GB are its heterogeneity, the high proliferative rate, infiltration into the cerebral parenchyma (2), resistance to treatment (3-5), and high vascularization (6). The modest outcomes of anti-angiogenic strategies in GB patients (7) and the lack of

understanding of how tumors modify endothelial cells (EC) behavior have increased the interest in studying GB-EC molecular interactions to identify alternative angiogenic targets for the development of new therapeutic perspectives.

The blood-brain barrier (BBB) is a complex structure formed by highly specialized brain microvascular endothelial cells (EC) with specific occlusive junctions (8, 9). Like other solid tumors, GB response to hypoxia involves the regulation of growth factors, chemokines and proteases, which induce alterations in the vessel structure by inducing the proliferation and migration of EC to form new blood vessels from pre-existing vessels (10). Angiogenesis in GB occurs at a high rate and also results in the aberrant and subfunctional architecture of the tumor vasculature (11, 12). In addition to EC-dependent angiogenesis, vascular mimicry also contributes to GB vascularization, although to a lesser extent (13). These vascular-like channels can be formed independently of EC *via* the transdifferentiation of GB stem cells (GSCs) into pericytes (PC) or smooth muscle cells (SMC). In contrast, in the presence of EC, GSC-differentiated PC/SMC cells can interact intimately with EC to facilitate angiogenesis and produce more stable vessels, which perfuse tumors more efficiently (14, 15). These angiogenic processes highlight the idiosyncrasies and complexity of GB angiogenesis, which may influence tumor EC in specific ways. Therefore, studies of the behavior of EC in the context of GB angiogenesis are important.

The principal and best-described angiogenic factor is vascular endothelial growth factor (VEGF), which has at least 6 isoforms in humans that are important for both embryonic development and tumor growth (16). These growth factors can induce survival, proliferation and migration of EC (17, 18). VEGFs are highly upregulated in GB, and their receptors are overexpressed in tumor vessels (13, 19, 20). VEGF-A is synthesized in massive quantities in gliomas, whereas other members of this family, such as VEGF-C and VEGF-D, are

*Correspondence to:* Prof. Valeria Pereira Ferrer. Department of Cellular and Molecular Biology, Institute of Biology, Fluminense Federal University, 30, Mario Santos Braga Street – Downtown, Niteroi, Rio de Janeiro, Brazil. Tel: +55 2126292261, e-mail: ferrervp@gmail.com

**Key Words:** Angiogenesis, endothelial cells, glioblastoma, cell crosstalk, MMP-9, CXCR4.

produced at much lower levels (20, 21). VEGF-A gradients induce the upregulation of the tyrosine kinase receptors VEGFR-2 and -3 in tip cells located at the most distal ends of sprouting capillaries (22-24). VEGF-A also induces the expression of the Notch ligand Dll4 on tip cells, which, by lateral inhibition, induces adjacent cells expressing Notch to become stalk cells. This ultimately provides negative feedback for VEGFR signaling by upregulating VEGFR-1 and inhibiting VEGFR-2 and -3 expression in stalk cells (24-27).

WNT family members are secreted proteins. In humans, the family consists of 19 members that regulate cell proliferation, differentiation, motility and fate in many stages of tumorigenesis. WNT binds to both G-protein-coupled transmembrane receptors (GPCRs) called Frizzled (Fz) and to receptors-related-to-low-density-lipoprotein (LRPs), which transduce their signals through  $\beta$ -catenin-dependent (canonical) or  $\beta$ -catenin-independent intracellular pathways (not canonical) (28). WNT5a signaling is involved in the development of various cancers, by contributing to angiogenesis and activating  $\beta$ -catenin-dependent or -independent pathways in various EC and tumor cell lines (28-30).

Chemotactic cytokines, a large superfamily of small peptides that signal through G-protein-coupled receptors (GPCRs), are another important group of molecules that are involved in angiogenesis. These receptors act *via* heterotrimeric G-proteins or through survival proteins such as arrestin to regulate a diverse set of signal-transduction pathways related to cell survival, proliferation and migration (2, 31). The stromal cell-derived factor 1 (SDF-1 or CXCL12)–CXCR4/7 axis drives the hypoxia-dependent angiogenesis and invasiveness of GB precursor cells. CXCL12 stimulates VEGF secretion in CXCR4-expressing CSCs cells of GB, which promotes tumor angiogenesis *via* PI3K/AKT signaling (32, 33). The function of CXCR4 has been linked to sprouting angiogenesis, as it is expressed in tip cells, and it can mediate VEGF expression through the transcription factor Yin Yang 1 or independently of the VEGF pathway (34-36). CXCR7, in turn, is highly expressed in tumor EC, microglial, and GB cells (37). Although CXCR7 has been shown to be highly expressed in the blood vessels of several tumors, its function in EC is only beginning to be understood (38). Increased expression of CXCR7 in microvascular EC during hypoxia favors CXCL12-induced glioma cell migration, which facilitates the binding of CXCL12 to EC and the activation of CXCL12-mediated cell crossing through the endothelium (36). In addition, CXCR7-targeted siRNA inhibits migration, tube formation and resistance to serum starvation in tumor EC (38).

Finally, matrix metalloproteinase 9 (MMP-9), also known as type IV collagenase, gelatinase or gelatinase B, is a matrixin, which is a class of enzymes that belong to the zinc-metalloproteinase family that are involved in the degradation of the extracellular matrix (ECM) (39). Endothelial barrier damage is associated with enhanced matrix MMP-9 activity,

which is known to mediate claudin-5 disruption (40). Furthermore, proteases such as MMP-9 can release growth factors bound to ECM and promote angiogenesis (41). MMP-9 has been shown to be associated with the migration of human brain EC and tubulogenesis (42, 43). Several signaling pathways culminate in increased expression of MMPs in gliomas. These include VEGF (44), WNT-5a (45) and CXCR4 pathways, which contribute to cell migration and secretion of MMPs, including gelatinases (46).

We have analyzed whether GB could influence proliferation and migration, which are key processes in angiogenesis, of human brain vascular EC (HBMEC). Very little is known about the angiogenic molecules produced and secreted by the EC in GB because most studies have focused on the pro-angiogenic profile of molecules secreted by the tumor cells. Therefore, we analyzed how GB factors influence the profile of the expression, protein levels and/or localization of important angiogenic factors and some of their receptors in HBMEC, which may be associated with the proliferation and migration of these ECs.

## Materials and Methods

**Cell culture.** Human brain microvascular endothelial cells (HBMEC) were cultured in the presence or absence of GB-conditioned media (GB-CM) (47), which comprised a mixture of CM from GBM02 and GBM11 cells that are patient-derived GB cells and were established in our laboratory as previously described (48). Both endothelial and GB cells were cultured in DMEM/F-12 medium (Dulbecco's Modified Eagle Medium) supplemented with 3.5 mg/ml glucose, 0.1 mg/ml penicillin, 0.14 mg/ml streptomycin, and 10% fetal bovine serum (FBS). To produce the CM, 75% confluent GB cells were incubated with serum-free DMEM/F-12 for 72 h. This medium was collected and filtered through a 0.2  $\mu$ m membrane. After the EC had achieved ~75% confluence, they were plated (the number of cells is specified in each assay) and treated with serum-free medium or with the pooled GB-CM (GB-CM: 25% CM from GBM11, 25% CM from GBM02 and 50% of fresh media) for 24, 48 or 72 h. The cells were maintained in a humidified atmosphere of 5% CO<sub>2</sub> at 37°C and were routinely tested for mycoplasma contamination (LT07-710 4C Reagent Mycoalert Plus, Lonza®, Basel, CH).

**Proliferation assay.** Proliferation was analyzed using a BrdU incorporation assay. HBMEC were plated at 3×10<sup>5</sup> cells/well in triplicate in a 96-well plate. The cells were treated with DMEM/F12 or GB-CM and were incubated for 24, 48 or 72 h at 37°C in a humidified atmosphere (5% CO<sub>2</sub>). The BrdU assay was performed according to the manufacturer's protocol (Cell Proliferation ELISA for BrdU, Roche®, Basel, CH). The BrdU labeling solution was added to the cultures for 50 min or 6 h (49) before completing each treatment (24, 48 or 72 h) to allow incorporation. The plate was protected from light and incubated in a humidified atmosphere (37°C, 5% CO<sub>2</sub>). After the incubation period, the culture medium was removed, and 100  $\mu$ l of FixDenat solution was added to each well. The samples were incubated for 30 min at room temperature. After this time, the reagent was removed, and BrdU POD-working solution (antiBrdU-FLUOS) was added and incubated for 1 h and 40

min. After washing three times with 1x PBS, 50 µl of the substrate solution were added and incubated for 3 min with stirring. The stop solution (H<sub>2</sub>SO<sub>4</sub>) was then added, and the plate was incubated for 5 min with shaking. The colorimetric analyses were performed by determining the absorbance at 690 nm using a Victor 3 1420 multilabel plate reader (PerkinElmer, Waltham, Massachusetts, US). The analyses were performed in four independent experiments.

**Scratch assay.** The migration capability of HBMEC was evaluated using a scratch assay. Two wells of a 24-well plate were used for each time point. To achieve a confluent EC monolayer,  $4 \times 10^5$  cells were plated in each well in serum-free conditions. Six hours later, 10 µM cytosine arabinoside (Ara-C) was added to inhibit proliferation of these cells, and the cultures were maintained for 24 h. Afterwards, a “wound” was made by scratching the monolayer with a 10 µl pipette tip in a straight line. Any debris and displaced cells were removed by gently washing the well three times with DMEM/F12. Subsequently, the cells were treated or not treated with GB-CM for 0, 24 and 48 h. To document the cell migration and compare the EC migration patterns in the samples, digital images from the center of each well were taken at a magnification of 10x. A CCD camera (Nikon Eclipse, Nikon, Shinagawa, Tokyo, JP) was used for the image acquisition. The width of each scratch was measured with Fiji for ImageJ software (version 1.52). The wound area comparisons were made using the 0 h values as the basis and plotting the respective areas for each condition at 24 or 48 h. Three independent experiments were performed.

**Western blotting.** HBMEC were cultured in plates and treated with GB-CM or control media for 24 h ( $4.2 \times 10^6$  cells/plate), 48 h ( $2.1 \times 10^6$  cells/plate) and 72 h ( $1.4 \times 10^6$  cells/plate). The cells were then washed with 1x PBS and detached using a cell scraper, after which 1x RIPA was added (20 mM Tris-HCl pH 7.5, 150 mM NaCl, 1 mM Na<sub>2</sub>EDTA, 1% NP-40, 1% sodium deoxycholate) that contained 1x protease inhibitors (S8830 Sigma Aldrich®, St. Louis, MO, USA). The lysates were sonicated 2 times for 10 s using a Ultrasonic® cell disruptor (Ultrasonic, Indaiatuba, São Paulo, BR) and then centrifuged at 4°C and  $10,000 \times g$  for 30 min. The supernatants were analyzed for protein content using a Bradford Bio-Rad Protein Assay kit (Cat n° #500-0006, BioRad®, Benicia, CA, US). Western blotting was performed as described by Towbin *et al.* (1979) with minor modifications (50). For immunodetection of proteins, 80 or 100 µg of total protein lysate was separated by electrophoresis in 8, 10 or 12% SDS polyacrylamide gels and transferred to polyvinylidene difluoride (PVDF) membranes. The PVDF membranes were then blocked with 5% nonfat milk in Tris-buffered saline with 0.1% Tween-20 (TBS-T) for 1 h and then incubated with specific primary antibodies overnight at 4°C. The primary antibodies used were anti-VEGF-A (1:1000, 437241 Abcam®, Cambridge, UK), anti-MMP-9 (1:1000, 436265 Abcam®, Dallas, TX, US), anti-CXCR4 (1:500, 9046 Santa Cruz Biotechnology®, Dallas, TX, US), anti-CXCR7 (1:1000, 117836 Abcam®), anti-WNT-5a (1:1000, 2392 Cell Signaling Technology®, Danvers, MA, USA), and anti- $\alpha$ -tubulin (1:2000, A11126 Sigma-Aldrich®). The membranes were washed with 0.1% TBS-T and incubated in 1:2000 Goat Anti-Mouse IgG (H + L) (G-21040 Thermo Fisher Scientific®, Waltham, MA, USA) or Goat Anti-Rabbit IgG (H + L) (G-21234 Thermo Fisher Scientific®) secondary antibody for 2 h. The bands were detected using chemiluminescence (ECL): West Pico Chemiluminescent Supersignal Developer Solutions Substrate® (34077 Thermo Fisher Scientific®) and Supersignal West Femto Maximum Sensitivity

Substrate® (34095 Thermo Fisher Scientific®) using a ChemiDoc MP imaging system (BioRad®, Benicia, CA, USA). The densitometry analyses were performed using ImageJ software (version 1.52), and the ratio between the immunodetected protein and the loading control ( $\alpha$ -tubulin) was calculated. As a positive control for the primary antibody specificity, GBM02 or GBM11 cells were used (data not shown) because GB cells secrete large quantities of the angiogenic factors analyzed (51-53). The analyses were performed using at least three biological replicates.

**Immunocytochemistry.** HBMEC were cultured on coverslips in a 24-well plate:  $5 \times 10^4$  for the time point of 24 h,  $2.5 \times 10^4$  for the time point of 48 h, and  $1.25 \times 10^4$  for the time point of 72 h. After incubation in the absence or presence of GB-CM at different time points, the cells were fixed with 4% paraformaldehyde (PFA)/PBS for 20 min, permeabilized with 0.1% Triton X-100/PBS, and blocked with 5% BSA/PBS for 1 h. For the immunofluorescent analysis of the localization of the angiogenic factors in the EC, the coverslips were incubated overnight at 4°C with anti-VEGF-A (1:500, 437241 Abcam®), anti-CXCR4 (1:250, 9046 Santa Cruz Technology®), anti-CXCL12 (16 µg/ml, MAB 350 R&D System®, Minneapolis, Minnesota, US), or anti-MMP-9 (1:500, 436265 Abcam®). Thereafter, the cells were washed with 1x PBS and incubated with secondary antibodies conjugated with Alexa Fluor: goat anti-rabbit IgG 488 1:250 (A-11008 Life Technologies®, Carlsbad, CA, USA) or Alexa Fluor® goat anti-mouse IgG 488 1:250 (A-11059 Life Technologies®) for 1 h and 30 min at room temperature. The coverslips were then washed with 1x PBS, stained with DAPI (4',6-diamino-2-phenylindole) at 1 µl/ml (D9542 Sigma-Aldrich®), and mounted on glass slides using Fluoromount-G®. Negative controls were prepared using the secondary antibodies. The cells were imaged at 63x using a DMi8 advanced fluorescence microscope (Leica Microsystems, Wetzlar, Germany) and analyzed with Leica LA SAF Lite. The images were processed using the software Fiji for ImageJ software version 1.52 (Wayne Rasband, National Institutes of Health, MD, USA). The analyses were performed using three biological replicates.

**qRT-PCR.** Total RNA was extracted from HBMEC using the TRIzol method (15596018 Life Technologies®) according to the manufacturer's instructions. One microgram of total RNA, Oligo(dT) primer 50 µM (58862 Life Technologies®), and High-Capacity cDNA Reverse Transcription Kit (4368814, Applied Biosystems®, Foster City, CA, USA) were used to perform the cDNA synthesis. We added 30 ng of cDNA per well and the Power Sybr Green Master Mix (4368706, Thermo Fisher Scientific) in triplicate in a 96-well plate (MLL9651, BioRad®). The reactions were run in a C1000 Touch Thermo Cycler (BioRad®), and  $\beta$ -actin was used as the endogenous gene control. The GBM02 cDNA was used as a positive control for amplification (data not shown). The analysis of relative gene expression (fold change) was conducted using the Pfaffl method (54).  $\beta$ -Actin was used as the endogenous gene control, and untreated samples were used as the control for each time point. The analyses were performed using two biological replicates. The primers used were as follows: total VEGF Forward (5'-TTCGGAACCAGATCTCTCACC-3'); total VEGF Reverse (5'-TTCGGAACCAGATCTCTCACC-3'); CXCR4 Forward (5'-GCC TTA TCC TGC CTG GTA TTG TC-3'); CXCR4 Reverse (5'-GCG AAG AAA GCC AGG ATG AGG AT-3');  $\beta$ -actin Forward (5'-ATGAAGATCAAGATCATTGCTCCT-3');  $\beta$ -actin Reverse (5'-ATGAAGATCAAGATCATTGCTCCT-3').

**Semiquantitative PCR.** WNT5a and MMP-9 gene expression in the HBMEC were analyzed using a semiquantitative method. After running the reactions in the C1000 Touch Thermo Cycler as described above, the samples were applied to an 8% acrylamide gel. A 100 bp DNA ladder was used as base pair marker (15628019, Invitrogen™). The gel was run at 75 v for 2 h and then was stained for 1 h with the UniSafe Dye (20,000 x) (UNI\_SRO1031, Uniscience do Brasil, Osasco, São Paulo, BR) with stirring. The images were acquired using a ChemiDoc™ Imaging System (Bio-Rad®), and the bands were quantified using the Fiji-ImageJ® program (version 1.52). The analyses were performed using two biological replicates. The primers used were as follows: MMP-9 Forward (5'-TTGACAGCGACAAGAAGTGG-3'); MMP-9 Reverse (5'-TCACGTCGTCCTTATGCAAG-3'); WNT5a Forward (5'-GGGAGGTTGGCTTGAACATA-3'); WNT5a Reverse (5'-AGGGCTCAGTGTGAAGAGGA-3');  $\beta$ -actin Forward (5'-ATGAAGATCAAGATCATTGCTCCT-3');  $\beta$ -actin Reverse (5'-ATGAAGATCAAGATCATTGCTCCT-3').

**Statistics.** The data are represented as the mean values and were analyzed for statistical significance using the paired sample *t*-test. The derived *p*-value levels are shown with stars indicating the significance: \**p*<0.05. The analyses for the qRT-PCR and semiquantitative PCR were performed using GraphPad online.

## Results

**HBMEC migration, but not proliferation, was increased in the presence of GB-CM.** Since GB are highly vascularized tumors, we examined whether the tumor-secreted factors would influence the proliferation and migration of EC. We tested whether GB-CM was able to modulate HBMEC proliferation using the BrdU incorporation method. The HBMEC proliferation rate was not altered following treatment with GB-CM at the time points analyzed (24, 48 and 72 h) (Figure 1A). We performed the scratch assay to evaluate whether GB-CM modify the migration rate of HBMEC. We observed that migratory rate of HBMEC was increased in the presence of GB-CM (\**p*<0.05) at 48 h (Figure 1B).

**The levels of MMP-9 in the HBMEC were increased following treatment with GB-CM.** We analyzed whether treatment with GB-CM would modulate MMP-9 levels in EC. The enzyme MMP-9 was detected in HBMEC extracts at all time points analyzed (Figure 2A). Specific bands were detected at ~92 kD. The levels of MMP-9 in HBMEC treated with GB-CM for 48 h or 72 h were significantly increased (\**p*<0.05) compared to those in HBMEC control (Figure 2A).

We further determined the subcellular localization of MMP-9 in HBMEC using immunocytochemistry. We observed punctiform labeling throughout the HBMEC cytosol at all time points analyzed. There was a significant increase in MMP-9 levels (*p*<0.05) when HBMEC were treated with GB-CM for 72 h compared to control (Figure 2B).

We also analyzed the MMP-9 mRNA expression levels. We detected bands of ~200 bp, which demonstrated the specificity for MMP-9 cDNA amplification. There was no statistically significant difference in MMP-9 mRNA levels between HBMEC treated with GB-CM (Figure 2C) compared to controls.

**An early mRNA level rise was followed by later increase in CXCR4 protein in GB-CM-treated HBMEC.** Given the importance of CXCL12 in the angiogenesis process and of CXCR4 expression in migrating endothelial tip cells, we analyzed the gene expression, protein levels and/or cellular location of this chemokine and its receptors CXCR4 and CXCR7 in HBMEC treated with GB-CM or control medium.

The qRT-PCR analysis indicated sustained early changes in the fold expression CXCR4 mRNA levels in the GB-CM-treated HBMEC compared to the control. The mRNA levels of CXCR4 increased 3-fold at 24 h and 2.4-fold at 48 h but then decreased to almost null levels at 72 h compared to the control (Figure 3A). We next analyzed CXCR4 and CXCR7 receptor levels using western blotting. Specific bands were detected in both HBMEC treated with GB-CM and untreated cells at all time points. We observed two bands for CXCR4 and CXCR7 at ~50 kD. We observed an increase in CXCR4 in HBMEC that were treated with GB-CM for 72 h (\**p*<0.05) (Figure 3B) compared to the control whereas the levels of CXCR7 protein were not altered when HBMEC were treated with GB-CM (Figure 3B).

Next, the subcellular localization of CXCR4 and its ligand CXCL12 in HBMEC that were treated with GB-CM or the control medium was analyzed by immunocytochemistry. We observed a punctiform nuclear labeling and a weaker punctiform cytosolic labeling of CXCR4, as shown in Figure 3C. Regarding CXCL12 profile, a punctiform cytoplasmic labeling apparently with a perinuclear concentration was observed (Figure 3D). No differences were observed regarding the levels of CXCR4 and CXCL12 by immunohistochemistry between the cells that were treated with GB-CM compared with the control cells at all time points analyzed.

**VEGFs and VEGFR2 were not affected following treatment of HBMEC with GB-CM.** We analyzed the protein levels, gene expression or subcellular localization of VEGF-A, total VEGF, and VEGFR2 in GB-CM-treated HBMEC. Specific bands of VEGF-A were visualized at ~40 and 50 kD in HBMEC that were treated with GB-CM as well as in the control cells (Figure 4A). The levels of VEGF-A protein in the cells that were treated with GB-CM did not differ from that of the control cells (Figure 4A and B). Consistent with this observation, the total VEGF gene expression in the GB-CM-treated HBMEC was not significantly different from that of the control (Figure 4C).

When we analyzed the levels of VEGFR2 and observed specific bands at ~75 kD that correspond to a shorter isoform containing only the extracellular domain of the receptor (55).

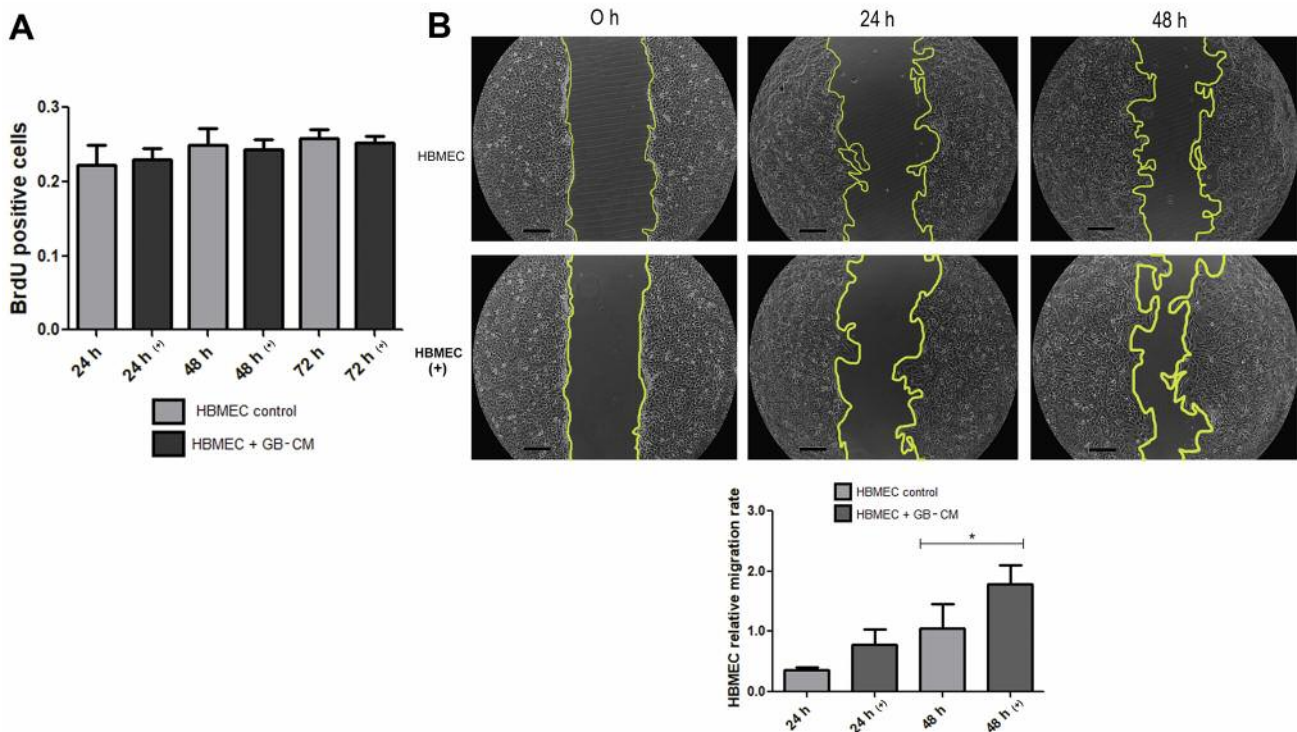


Figure 1. HBMEC migration, but not proliferation, was modified by GB-CM treatment. (A) The proliferation rate is expressed by the number of HBMEC that incorporated BrdU. The HBMEC control is represented by the light gray bars, and the HBMEC that were treated with GB-CM are represented with (+) and by dark gray bars. The HBMEC proliferation was not changed when these cells were treated with GB-CM for 24, 48 or 72 h. (B) Migration rate analysis by scratch assay. After wounding the cell monolayer, the HBMEC were treated or not with GB-CM. The monolayer wound areas were measured at 0, 24 and 48 h after treatment. Greater migration of the HBMEC that were treated with GB-CM for 48 h was observed compared to the untreated cells (\* $p < 0.05$ ). The scale bar corresponds to 1  $\mu$ m. Statistical analysis was performed to compare the wound area in the GB-CM-treated cells with the wound area of untreated cells relative to the area at 0 h. The analysis was performed using results from duplicates for each condition in three independent experiments. The bars correspond to the mean  $\pm$  standard deviation values.

The VEGFR2 protein levels were not significantly altered in HBMEC that were treated with GB-CM compared to control (Figure 4D).

*WNT5a* was not affected following treatment of HBMEC with GB-CM. We next assayed for the levels of the *WNT5a* gene expression and protein in HBMEC treated with GB-CM compared to untreated cells.

WNT5a was detected in both treated and untreated HBMEC. WNT5a-specific bands were detected at ~ 45 kD at all time points analyzed. As shown in Figure 5A, incubation of HBMEC with GB-CM did not significantly alter WNT5a levels at any of the analyzed time points. To complement the protein analysis, we also analyzed the WNT5a mRNA levels by performing semiquantitative PCR. We detected bands between 200 and 300 bp, which demonstrated WNT5a-specific cDNA amplification (Figure 5B). *WNT5a* gene expression was not altered following treatment of HBMEC at the various time points in comparison to the control cells.

## Discussion

Angiogenesis is essential for efficient GB growth and expansion (56). Several factors that are secreted by both tumor cells and blood vessel EC have been reported to participate in the process of angiogenesis in tumors (37, 57-59). Among these factors, VEGF (60-62), WNT (58, 63), metalloproteases (64, 65) and chemokines (20, 66) are prominent. However, regarding the molecular communication between GB and blood vessel EC, few studies have focused specifically on the effects of factors secreted by GB on the expression of angiogenic factors by EC (52).

In the present study, we analyzed whether factors secreted by GB would influence EC in brain microvasculature *in vitro*. To answer this question, we first established a model of molecular communication between GB and HBMEC cells. The GBM02 cells were derived from a secondary GB recurrent tumor that had not been treated with chemotherapy or radiotherapy (67). The GBM11 cells were derived from a recurrent GB that had previously been treated with

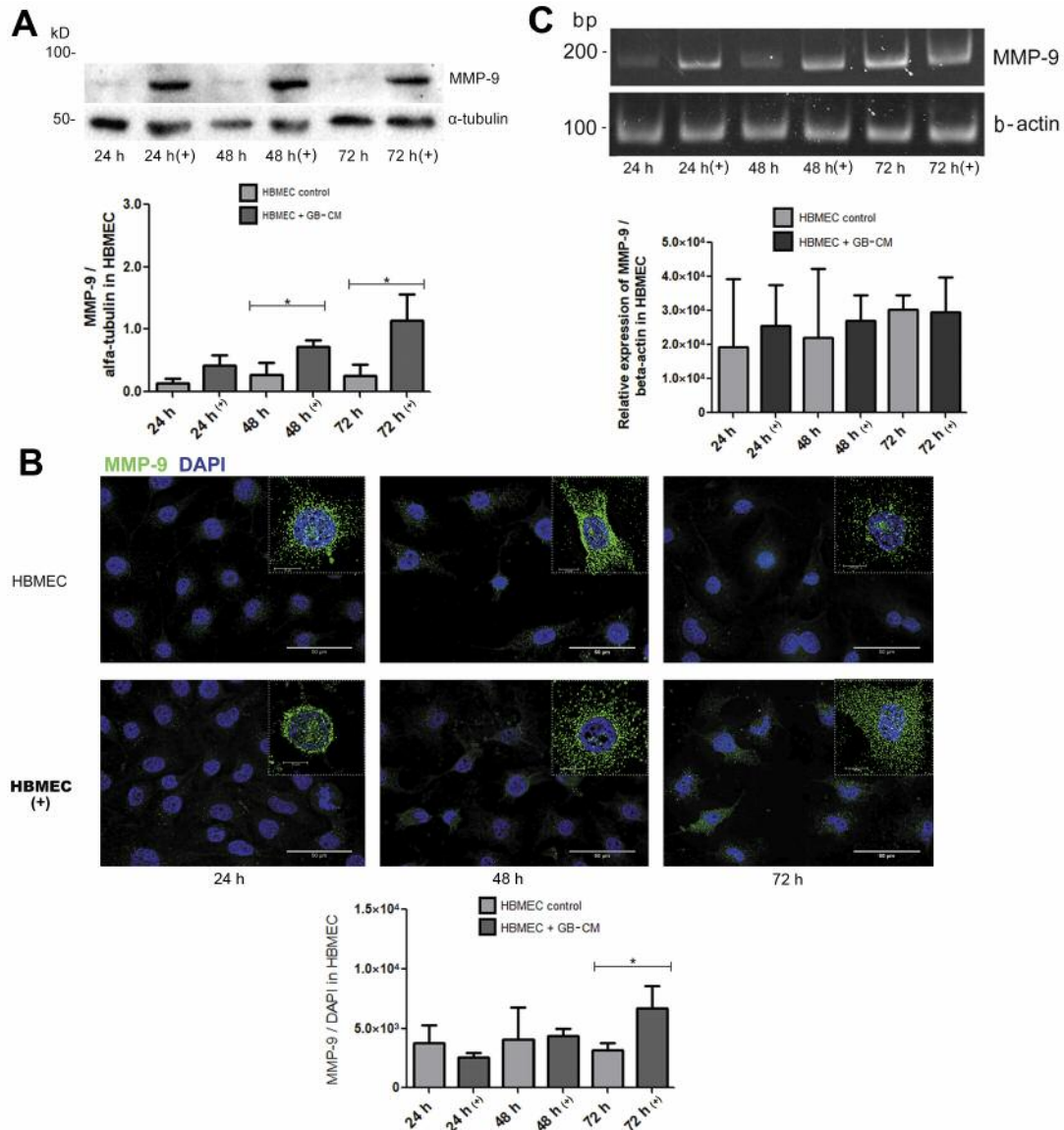


Figure 2. HBMEC treated with GB-CM increased MMP-9. HBMEC that were treated with GB-CM are represented by (+). (A) MMP-9 protein analysis by western blot. The densitometric ratios between the MMP-9 band and the loading control ( $\alpha$ -tubulin) are plotted in the graph. Comparisons of the levels of MMP-9 in the treated and untreated cells showed a significant increase ( $*p<0.05$ ) after 48 h and 72 h of treatment. (B) MMP-9 cell localization. MMP-9 (green) and the nuclei (DAPI, blue). The densitometric ratios of total MMP-9 signal per total DAPI signal are plotted in the graph. A significant increase in MMP-9 immunolabeling was observed in the cells that were treated with GB-CM for 72 h compared to the untreated cells. The scale bar represents 50  $\mu$ m, and the scale bar for zoomed cells (in dashed square) represents 10  $\mu$ m. The analysis was performed using the data from three independent experiments. (C) MMP-9 relative gene expression by semiquantitative PCR. Specific bands at  $\sim 200$  bp were detected. The densitometric ratios between MMP-9 and endogenous gene ( $\beta$ -actin) amplified bands are plotted in the graph. There was no difference in MMP-9 gene expression in the treated cells compared to the controls. The results from two biological replicates with technical triplicates were used for this analysis. The statistical analysis was performed using the paired samples t-test ( $*p<0.05$ ). The bars correspond to the mean  $\pm$  standard deviation values.

chemotherapy and radiotherapy and was resistant to chemotherapy (4). Due to the heterogeneity of GB (68), we have chosen to work with different GB cells. To minimize biological variability and obtain results that could be generalized, we treated HBMEC with a mixture of CM derived from both cell lines (GB-CM) (47). The simulation of cellular

communication through CM treatment is a well-established method that has been used in several studies (67, 69, 70).

Our study investigated whether GB-CM influence HBMEC proliferation. We did not observe a difference in the proliferation rate of GB-CM-treated HBMEC at the selected time points. However, HBMEC proliferation was increased

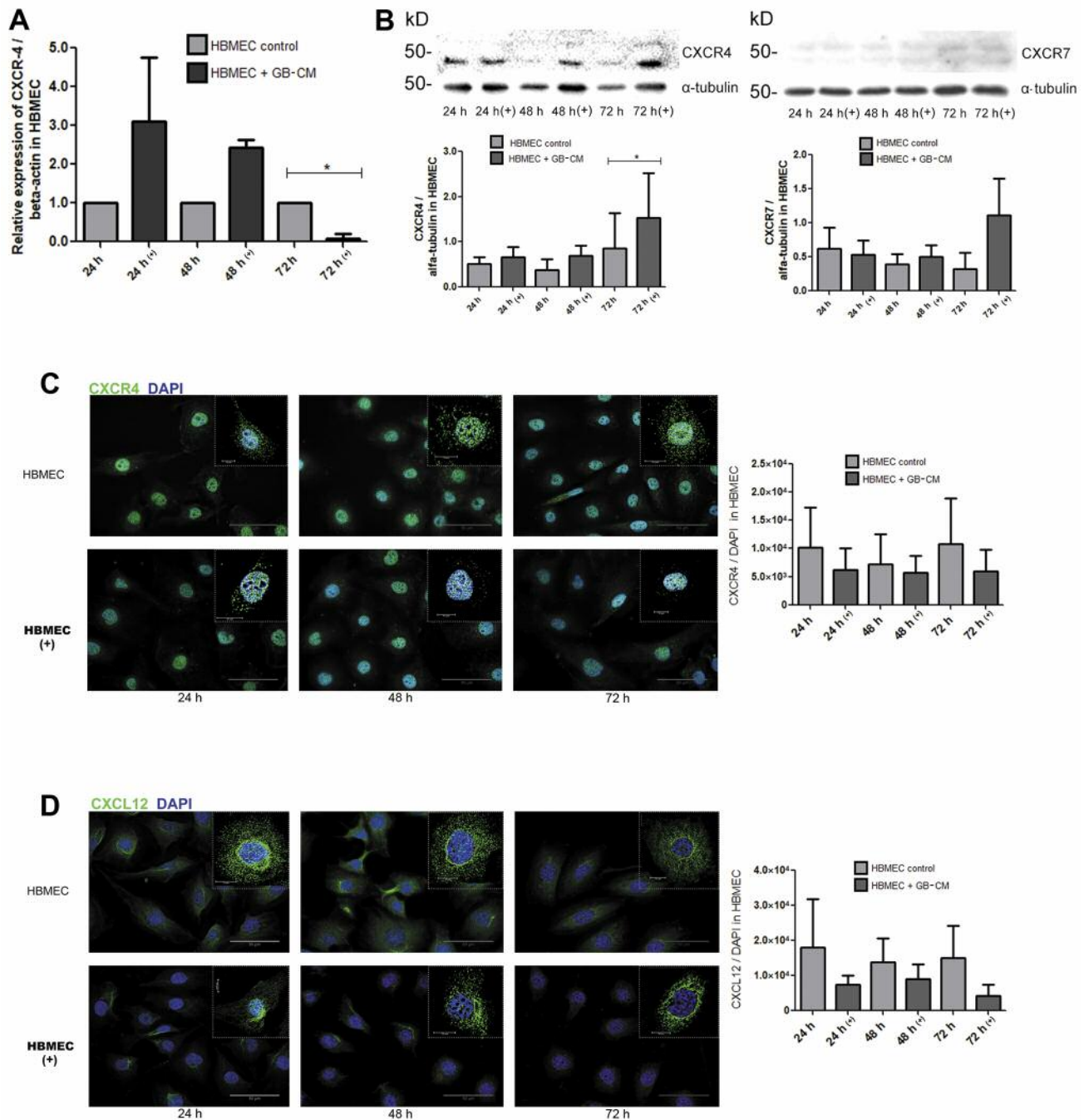


Figure 3. The CXCL12-CXCR4-CXCR7 axis in HBMEC treated with GB-CM. HBMEC that were treated with GB-CM are represented by (+). (A) CXCR4 gene expression analysis. CXCR4 expression was significantly decreased in HBMEC treated with GB-CM for 72 h compared to the control. The relative gene expression was analyzed using data from the cells that were treated with GB-CM compared with the untreated cells.  $\beta$ -actin gene was used as the gene control. The analysis was performed with data from two independent experiments using technical triplicates. (B) CXCR4 protein analysis by western blot. The densitometric ratios between the CXCR4 band and the loading control ( $\alpha$ -tubulin) are plotted in the graph. We observed a significant increase of CXCR4 in the HBMEC that were treated with GB-CM for 72 h compared to the control. Western blot and respective densitometric ratio analysis showed no difference in the amount of CXCR7 in the cells that were treated with GB-CM compared to control cells.  $\alpha$ -Tubulin was used as a loading control and three biological replicates were performed. (C) CXCR4 demonstrated a cytoplasmic and nuclear labeling. There was no difference in the quantification of CXCR4 immunolabeling between treated and nontreated HBMEC. (D) CXCL12 labeling pattern. There was no difference in the quantification of CXCL12 immunolabeling between treated and nontreated HBMEC. CXCR4 or CXCL12 labeling (green) and nuclear labeling (DAPI, blue). The scale bar represents 50  $\mu$ m, and the scale bar for zoomed cells (in dashed square) represents 10  $\mu$ m. The analysis was performed using data from three independent experiments (\* $p$ <0.05). The bars correspond to the mean  $\pm$  standard deviation values.

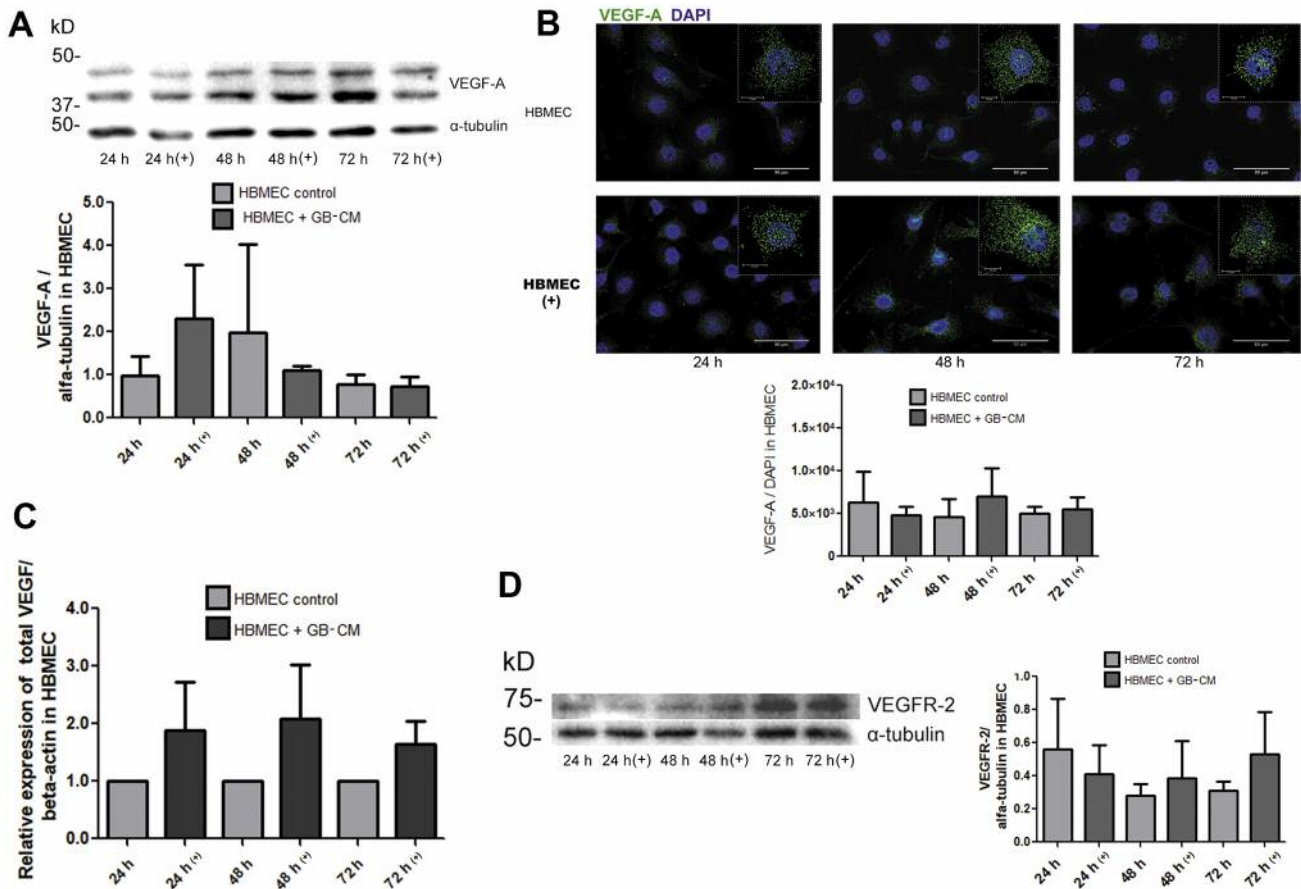


Figure 4. VEGFs and VEGFR-2 levels were not modified in HBMEC that were treated with GB-CM. The HBMEC that were treated with GB-CM are identified by (+). (A) VEGF-A protein analysis. Bands at ~40 and 50 kD are observed. There was no difference in the levels of VEGF-A. (B) VEGF-A cytolocalization. VEGF-A labeling (green) and the nuclei (DAPI, blue). There was no difference in VEGF-A immunolabeling quantification. The scale bar represents 50  $\mu$ m, and the scale bar for zoomed cells (in dashed square) represents 10  $\mu$ m. (C) Total VEGF gene expression analysis. Relative analysis was performed using total VEGF mRNA compared to mRNA of  $\beta$ -actin using untreated samples as controls. We did not observe significant differences in VEGF gene expression. (D) VEGFR-2 protein analysis. VEGFR-2 was detected in HBMEC at ~75 kD. There was no difference in the levels of VEGFR-2 between treated and untreated HBMEC. The analysis was performed using results from three biological replicates for western blotting and immunocytochemistry analysis, and from two independent experiments for qRT-PCR, with technical triplicates. The bars correspond to the mean  $\pm$  standard deviation values.

when they were maintained in coculture with GB U87, as demonstrated by Ki-67 labeling (52). Moreover, Giusti and colleagues (2016) demonstrated that treatment with various concentrations of GB U251 extracellular vesicles (EV) that contained IL-6, IL-8, VEGF and CXCR4 increased HBMEC proliferation (53). It is noteworthy that concentrated EV were used in those studies. Therefore, the influence of GB or GB-derived molecules on EC proliferation requires further studies.

We observed a significant increase in the migration rates of the HBMEC that were treated with GB-CM compared to HBMEC controls. Our results corroborate that of Giusti and colleagues (2016), who observed increased migratory rates in HBMEC that were exposed to various concentrations of U251 EV (6 and 8  $\mu$ g/ml) (53).

Further, we analyzed which angiogenic factors were modulated in HBMEC following treatment with GB-CM. We analyzed the profile of protein or gene expression of important angiogenic factors that are involved in EC migration and proliferation.

Metalloproteases are zinc-dependent endopeptidases that mediate ECM degradation and dissociation. These enzymes are produced and secreted by both EC and GB cells, and they are important for both the invasive features of gliomas and for angiogenesis in these tumors (28, 71). We observed a significant increase in MMP-9 protein levels in the HBMEC that were treated with GB-CM. These data demonstrated that the factors secreted by the GB cells influenced HBMEC to modulate the levels of MMP-9. In agreement, Ngo and Harley

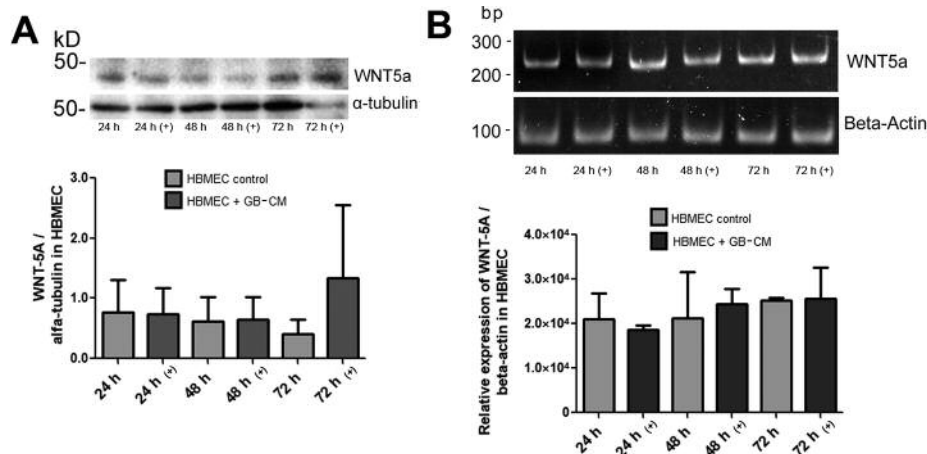


Figure 5. *WNT5a* gene expression and protein levels were not modified in HBMEC that were treated with GB-CM. The HBMEC treated with GB-CM are designated by (+). (A) Protein analysis of *WNT5a*. Bands at ~45 kD were detected in HBMEC at all time points and conditions analyzed. There was no difference of *WNT5a* in the HBMEC that were treated with GB-CM compared to the control.  $\alpha$ -Tubulin was used as a loading control. Three independent biological replicates were performed. (B) *WNT5a* expression was detected and quantified using semiquantitative PCR. *WNT5a* relative expression was determined in HBMEC that were treated with GB-CM and in nontreated cells. Specific bands between 200 and 300 bp were detected. The densitometric ratios between the amplified bands for *WNT5a* and the endogenous gene ( $\beta$ -actin) are plotted in the graph. No difference was observed. The results from two independent biological samples using technical triplicates were used in the analysis. The bars correspond to the mean  $\pm$  standard deviation values.

(2017) have also observed a significant increase in MMP-9 in their culture model: HUVEC (human umbilical vein endothelial cells) cocultured with human fibroblasts and GB U87 in a hydrogel (72). Kenig *et al.* (2010) observed increased MMP-9 levels in both U87 and HMEC-1 cells (human microvascular endothelial cells) under coculture conditions (52). These authors suggested that the presence of HMEC-1 resulted in increased invasion by the U87 cells that was mediated by positive regulation and MMP-9 secretion by both EC and tumor cells. However, it is noteworthy that the effects on the invasive potential of HMEC-1 co-cultivated with U87 cells were not examined in that study. Therefore, for the first time, our study demonstrates the parallel increase of MMP-9 and the migratory rate of EC exposed to GB-CM.

CXCL12 and its receptors CXCR4 and CXCR7 regulate several cellular functions, such as endothelial and tumor cell migration and angiogenesis. These proteins are overexpressed in malignant gliomas compared to normal tissues and are involved in tumor angiogenesis (34, 73). We have observed an early sustained increase in the CXCR4 mRNA levels. The inverse correlation between the protein and mRNA levels has been demonstrated in some studies. Different mechanisms act in mRNA and protein stabilization, and their levels might be in fact different (74). For instance, Tang *et al.* (2017) suggested that the relationship between CXCR4 mRNA and protein expression in EC is not strictly linear *in vitro* in hypoxic conditions (75). Nevertheless, we observed a significant increase in CXCR4 protein levels in HBMEC that were treated with GB-CM at 72h. We suggest that the modulation of MMP-9 and CXCR4 in ECs, in

addition to the GB-derived angiogenic factors, contributes to increased migration rates of HBMEC that we demonstrated with the scratch assay.

We did not observe a significant increase in either VEGF-A or total VEGF levels in the treated HBMEC at any of the time points analyzed. VEGF is a potent mitogen for EC, and it is the major growth factor involved in angiogenesis. The VEGF family members are essential for tumor angiogenesis (13) and VEGF is expressed by both EC and GB cells (76-79). Domigan *et al.* (2015) showed that EC are dependent on endogenous VEGF for survival (80). In the EC, VEGFs act through VEGFR-1 and VEGFR-2 tyrosine kinase receptors. In adulthood, VEGFR-2 is believed to be the signal transducer for physiological and pathological angiogenesis due to its high tyrosine kinase activity (81). We did not observe differences in VEGFR-2 (75 kD isoform) between the HBMEC that were treated with GB-CM and the control cells. Therefore, further studies are still necessary to clarify the role of VEGFR-2 isoform (82), and other VEGFR receptors in the EC and GB crosstalk.

The GB-derived secreted angiogenic factors may influence the migration of the ECs. Here, we cannot discard this hypothesis. Further *in vitro* and *in vivo* studies are necessary to explore the role of MMP-9 and CXCR4 synthesized by EC in the increased migration of HBMEC. However, we would like to highlight that the data we obtained by analyzing key angiogenic molecules in HBMEC matches the results of our migration and proliferation functional assays. We observed increases in MMP-9 and CXCR4 protein levels in HBMEC that were treated with GB-CM. Both of these factors are involved in migration and angiogenesis, consistent with the

migration rate in these cells. However, and consistent with the absence of changes in EC proliferation, we did not observe differences in molecules that are involved in EC proliferation, such as VEGF and WNT5a.

Anti-angiogenic therapy with bevacizumab was introduced to inhibit vascular endothelial growth factor (VEGF)-mediated tumor neovascularization in several cancers including GB (83). Unfortunately, the results from clinical trials did not meet expectations. Patients failed to respond to anti-angiogenic therapy or developed resistance (84). Recent evidence indicates that the dogma of tumor neovascularization that is solely dependent on VEGF pathway may be too simplistic (83). Limiting tumor angiogenesis has been a goal for anticancer therapy, but traditional growth factor-targeted anti-angiogenic treatments have had limited success. In recent years, it has increasingly been recognized that focusing on altered tumor EC metabolism might lead to compelling alternative anti-angiogenic strategies (85), which our study has accomplished.

## Conflicts of Interest

The Authors have no conflicts of interest to disclose regarding this study.

## Authors' Contributions

Designed the experiments: VF and DM. Conducted the experiments: LR, BG and TL. Supervised the involved scientists and discussed the obtained results: VF and CF. Wrote the manuscript: LR and VF. Edited the manuscript: CF, BG, DM and TL.

## Acknowledgements

The Authors would like to thank Prof. Vivaldo Moura-Neto for all the scientific support and Prof. Miguel Quartin for the assistance in the statistics. We also thank Dr. Tania Spohr and Prof. Juliana Coelho-Aguiar for the technical assistance in immunocytochemistry image acquisition. This study was supported by Coordenação de Aperfeiçoamento de Pessoal de Nível Superior (CAPES), Conselho Nacional de Desenvolvimento Científico e Tecnológico (CNPq), Fundação de Amparo à Pesquisa do Estado do Rio de Janeiro (FAPERJ) and Pró-Saúde Associação Beneficente de Assistência Social e Hospitalar.

## References

- Louis DN, Perry A, Reifenberger G, von Deimling A, Figarella-Branger D, Cavenee WK, Ohgaki H, Wiestler OD, Kleihues P and Ellison DW: The 2016 World Health Organization Classification of Tumors of the Central Nervous System: a summary. *Acta Neuropathol* 131: 803-820, 2016. PMID: 27157931. DOI: 10.1007/s00401-016-1545-1
- Ferrer VP, Neto VM and Mentlein R: Glioma infiltration and extracellular matrix : Key players and modulators. *Glia* 66: 1542-1565, 2018. PMID: 29464861. DOI: 10.1002/glia.23309
- Matias D, Balça-Silva J, Dubois LG, Pontes B, Ferrer VP, Rosário L, Do Carmo A, Echevarria-Lima J, Sarmiento-Ribeiro AB, Lopes MC and Moura-Neto V: Dual treatment with shikonin and temozolomide reduces glioblastoma tumor growth, migration and glial-to-mesenchymal transition. *Cell Oncol* 40: 24-261, 2017. PMID: 28401486. DOI: 10.1007/s13402-017-0320-1
- Balça-Silva J, Matias D, Do Carmo A, Dubois LG, Gonçalves AC, Girao H, Silva Canedo NH, Correia AH, De Souza JM, Sarmiento-Ribeiro AB, Lopes MC and Moura-Neto V: Glioblastoma entities express subtle differences in molecular composition and response to treatment. *Oncol Rep* 38: 1341-1352, 2017. PMID: 28714013. DOI: 10.3892/or.2017.5799
- Balça-Silva J, Matias D, Carmo AD, Sarmiento-Ribeiro AB, Lopes MC and Moura-Neto V: Cellular and molecular mechanisms of glioblastoma malignancy: Implications in resistance and therapeutic strategies. *Semin Cancer Biol* 58: 130-141, 2018. PMID: 30266571. DOI: 10.1016/j.semcancer.2018.09.007
- Wesseling P, Schlingemann RO, Rietveld FJR, Link M, Burger PC and Ruiter DJ: Early and extensive contribution of pericytes/vascular smooth muscle cells to microvascular proliferation in glioblastoma multiforme: An immuno-light and immuno-electron microscopic study. *J Neuropathol Exp Neurol* 54: 301-310, 1995. PMID: 7745429. DOI: 10.1097/00005072-199505000-00003
- Geraldo LHM, Garcia C, da Fonseca ACC, Dubois LGF, de Sampaio e Spohr TCL, Matias D, de Camargo Magalhães ES, do Amaral RF, da Rosa BG, Grimaldi I, Leser FS, Janeiro JM, Macharia L, Wanjiru C, Pereira CM, Moura-Neto V, Freitas C and Lima FRS: Glioblastoma therapy in the age of molecular medicine. *Trends Cancer* 5: 46-65, 2019. PMID: 30616755. DOI: 10.1016/j.trecan.2018.11.002
- Chatard M, Puech C, Perek N and Roche F: Hydralazine is a suitable mimetic agent of hypoxia to study the impact of hypoxic stress on *in vitro* blood-brain barrier model. *Cell Physiol Biochem* 42: 1592-1602, 2017. PMID: 28738383. DOI: 10.1159/000479399
- Abbott NJ, Patabendige AAK, Dolman DEM, Yusof SR and Begley DJ: Structure and function of the blood-brain barrier. *Neurobiol Dis* 37: 13-25, 2010. PMID: 19664713. DOI: 10.1016/j.nbd.2009.07.030
- Zhao C, Wang H, Xiong C and Liu Y: Hypoxic glioblastoma release exosomal VEGF-A induce the permeability of blood-brain barrier. *Biochem Biophys Res Commun* 502: 324-331, 2018. PMID: 29787762. DOI: 10.1016/j.bbrc.2018.05.140
- Alves TR, da Fonseca AC, Nunes SS, da Silva AO, Dubois LG, Faria J, Kahn SA, Viana NB, Marcondes J, Legrand C, Moura-Neto V and Morandi V: Tenascin-C in the extracellular matrix promotes the selection of highly proliferative and tubulogenesis-defective endothelial cells. *Exp Cell Res* 317: 2073-2085, 2011. PMID: 21740900. DOI: 10.1016/j.yexcr.2011.06.006
- Rupp T, Langlois B, Koczorowska MM, Radwanska A, Sun Z, Hussenet T, Lefebvre O, Murdamoothoo D, Arnold C, Klein A, Biniossek ML, Hyenne V, Naudin E, Velazquez-Quesada I, Schilling O, Van Obberghen-Schilling E and Orend G: Tenascin-C orchestrates glioblastoma angiogenesis by modulation of pro- and anti-angiogenic signaling. *Cell Rep* 17: 2607-2619, 2016. PMID: 27926865. DOI: 10.1016/j.celrep.2016.11.012
- Plate KH, Scholz A and Dumont DJ: Tumor angiogenesis and anti-angiogenic therapy in malignant gliomas revisited. *Acta Neuropathol* 124: 763-775, 2012. PMID: 23143192. DOI: 10.1007/s00401-012-1066-5
- Mei X, Chen YS, Chen FR, Xi SY and Chen ZP: Glioblastoma stem cell differentiation into endothelial cells evidenced through

- live-cell imaging. *Neuro Oncol* 19: 1109-1118, 2017. PMID: 28340100. DOI: 10.1093/neuonc/nox016
- 15 Shao R, Taylor SL, Oh DS and Schwartz LM: Vascular heterogeneity and targeting: the role of YKL-40 in glioblastoma vascularization. *Oncotarget* 6: 40507-40618, 2015. PMID: 26439689. DOI: 10.18632/oncotarget.5943
  - 16 Guo P, Xu L, Pan S, Brekken RA, Yang ST, Whitaker GB, Nagane M, Thorpe PE, Rosenbaum JS, Su Huang HJ, Caveness WK and Cheng SY: Vascular endothelial growth factor isoforms display distinct activities in promoting tumor angiogenesis at different anatomic sites. *Cancer Res* 61: 8569-8577, 2001. PMID: 11731444.
  - 17 Alon T, Hemo I, Itin A, Pe'er J, Stone J and Keshet E: Vascular endothelial growth factor acts as a survival factor for newly formed retinal vessels and has implications for retinopathy of prematurity. *Nat Med* 1: 1024-1028, 1995. PMID: 7489357. DOI: 10.1038/nm1095-1024
  - 18 Giordano A, D'Angelillo A, Romano S, D'Arrigo P, Corcione N, Bisogni R, Messina S, Polimeno M, Pepino P, Ferraro P and Romano MF: Tirofiban induces VEGF production and stimulates migration and proliferation of endothelial cells. *Vascul Pharmacol* 61: 63-71, 2014. PMID: 24751361. DOI: 10.1016/j.vph.2014.04.002
  - 19 Linhares P, Viana-Pereira M, Ferreira M, Amorim J, Nabico R, Pinto F, Costa S, Vaz R and Reis RM: Genetic variants of vascular endothelial growth factor predict risk and survival of gliomas. *Tumor Biol* 2018: 1-11, 2018. PMID: 29584591. DOI: 10.1177/1010428318766273
  - 20 Hattermann K and Mentlein R: Para- and autocrine mediators in the glioma microenvironment. In: *Glioma Cell Biology*. Hattermann K, Mentlein R (eds.). Springer Wien Heidelberg New York Dordrecht London, pp. 153-185, 2014.
  - 21 Jenny B, Harrison JA, Baetens D, Tille JC, Burkhardt K, Mottaz H, Kiss JZ, Dietrich PY, De Tribolet N, Pizzolato GP and Pepper MS: Expression and localization of VEGF-C and VEGFR-3 in glioblastomas and haemangioblastomas. *J Pathol* 209: 34-43, 2006. PMID: 16523449. DOI: 10.1002/path.1943
  - 22 Gerhardt H, Golding M, Fruttiger M, Ruhrberg C, Lundkvist A, Abramsson A, Jeltsch M, Mitchell C, Alitalo K, Shima D and Betsholtz C: VEGF guides angiogenic sprouting utilizing endothelial tip cell filopodia. *J Cell Biol* 161: 1163-1177, 2003. PMID: 12810700. DOI: 10.1083/jcb.200302047
  - 23 Tammela T, Zarkada G, Wallgard E, Murtomäki A, Suchting S, Wirzenius M, Waltari M, Hellström M, Schomber T, Peltonen R, Freitas C, Duarte A, Isoniemi H, Laakkonen P, Christofori G, Ylä-Herttuala S, Shibuya M, Pytowski B, Eichmann A, Betsholtz C and Alitalo K: Blocking VEGFR-3 suppresses angiogenic sprouting and vascular network formation. *Nature* 454: 656-660, 2008. PMID: 18594512. DOI: 10.1038/nature07083
  - 24 Benedito R, Rocha SF, Woeste M, Zamykal M, Radtke F, Casanovas O, Duarte A, Pytowski B and Adams RH: Notch-dependent VEGFR3 upregulation allows angiogenesis without VEGF-VEGFR2 signalling. *Nature* 484: 110-114, 2012. PMID: 22426001. DOI: 10.1038/nature10908
  - 25 Hellström M, Phng LK, Hofmann JJ, Wallgard E, Coultas L, Lindblom P, Alva J, Nilsson AK, Karlsson L, Gaiano N, Yoon K, Rossant J, Iruela-Arispe ML, Kalén M, Gerhardt H and Betsholtz C: Dll4 signalling through Notch1 regulates formation of tip cells during angiogenesis. *Nature* 445: 776-780, 2007. PMID: 17259973. DOI: 10.1038/nature05571
  - 26 Lobov IB, Renard RA, Papadopoulos N, Gale NW, Thurston G, Yancopoulos GD and Wiegand SJ: Delta-like ligand 4 (Dll4) is induced by VEGF as a negative regulator of angiogenic sprouting. *Proc Natl Acad Sci U S A* 104: 3219-3224, 2007. PMID: 17296940. DOI: 10.1073/pnas.0611206104
  - 27 Suchting S, Freitas C, Le Noble F, Benedito R, Bréant C, Duarte A and Eichmann A: The Notch ligand Delta-like 4 negatively regulates endothelial tip cell formation and vessel branching. *Proc Natl Acad Sci USA* 104: 3225-3230, 2007. PMID: 17296941. DOI: 10.1073/pnas.0611177104
  - 28 Kamino M, Kishida M, Kibe T, Ikoma K, Iijima M, Hirano H, Tokudome M, Chen L, Koriyama C, Yamada K, Arita K and Kishida S: Wnt-5a signaling is correlated with infiltrative activity in human glioma by inducing cellular migration and MMP-2. *Cancer Sci* 102: 540-548, 2011. PMID: 21205070. DOI: 10.1111/j.1349-7006.2010.01815.x
  - 29 Zeng A, Yin J, Li Y, Li R, Wang Z, Zhou X, Jin X, Shen F, Yan W and You Y: MiR-129-5p targets Wnt5a to block PKC/ERK/NF- $\kappa$ B and JNK pathways in glioblastoma. *Cell Death Dis* 9: 394-410, 2018. PMID: 29531296. DOI: 10.1038/s41419-018-0343-1
  - 30 Yao L, Sun B, Zhao X, Zhao X, Gu Q, Dong X, Zheng Y, Sun J, Cheng R, Qi H and An J: Overexpression of Wnt5a promotes angiogenesis in NSCLC. *Biomed Res Int*, 2014. PMID: 24999479. DOI: 10.1155/2014/832562
  - 31 Décaillot FM, Kazmi MA, Lin Y, Ray-Saha S, Sakmar TP and Sachdev P: CXCR7/CXCR4 heterodimer constitutively recruits  $\beta$ -arrestin to enhance cell migration. *J Biol Chem* 286: 32188-32197, 2011. PMID: 21730065. DOI: 10.1074/jbc.M111.277038
  - 32 Ping YF, Yao XH, Jiang JY, Zhao LT, Yu SC, Jiang T, Lin MCM, Chen JH, Wang B, Zhang R, Cui YH, Qian C, Wang JM and Bian XW: The chemokine CXCL12 and its receptor CXCR4 promote glioma stem cell-mediated VEGF production and tumour angiogenesis via PI3K/AKT signalling. *J Pathol* 224: 344-354, 2011. PMID: 21618540. DOI: 10.1002/path.2908
  - 33 Würth R, Bajetto A, Harrison JK, Barbieri F and Florio T: CXCL12 modulation of CXCR4 and CXCR7 activity in human glioblastoma stem-like cells and regulation of the tumor microenvironment. *Front Cell Neurosci* 8: 144, 2014. PMID: 24904289. DOI: 10.3389/fncel.2014.00144
  - 34 Strasser GA, Kaminker JS and Tessier-Lavigne M: Microarray analysis of retinal endothelial tip cells identifies CXCR4 as a mediator of tip cell morphology and branching. *Blood* 115: 5102-5110, 2010. PMID: 20154215. DOI: 10.1182/blood-2009-07-230284
  - 35 de Nigris F, Crudele V, Giovane A, Casamassimi A, Giordano A, Garban HJ, Cacciatore F, Pentimalli F, Marquez-Garban DC, Petrillo A, Cito L, Sommesse L, Fiore A, Petrillo M, Siani A, Barbieri A, Arra C, Rengo F, Hayashi T, Al-Omran M, Ignarro LJ and Napoli C: CXCR4/YY1 inhibition impairs VEGF network and angiogenesis during malignancy. *Proc Natl Acad Sci U S A* 107: 14484-14489. PMID: 20660740. DOI: 10.1073/pnas.1008256107
  - 36 Duda DG, Kozin S V, Kirkpatrick ND, Xu L, Fukumura D and Jain RK: CXCL12 (SDF1 $\alpha$ )-CXCR4/CXCR7 pathway inhibition: An emerging sensitizer for anticancer therapies? *Clin Cancer Res* 17: 2074-2080, 2011. PMID: 21349998. DOI: 10.1158/1078-0432.CCR-10-2636
  - 37 Hattermann K, Held-Feindt J, Lucius R, Muerköster SS, Penfold MET, Schall TJ and Mentlein R: The chemokine receptor CXCR7 is highly expressed in human glioma cells and mediates antiapoptotic effects. *Cancer Res* 70: 3299-3308, 2010. PMID: 20388803. DOI: 10.1158/0008-5472.CAN-09-3642

- 38 Yamada K, Maishi N, Akiyama K, Towfik Alam M, Ohga N, Kawamoto T, Shindoh M, Takahashi N, Kamiyama T, Hida Y, Taketomi A and Hida K: CXCL12-CXCR7 axis is important for tumor endothelial cell angiogenic property. *Int J Cancer* 137: 2825-2836, 2015. PMID: 26100110. DOI: 10.1002/ijc.29655
- 39 Benjamin MM and Khalil RA: Matrix metalloproteinase inhibitors as investigative tools in the pathogenesis and management of vascular disease. *EXS* 103: 209-279, 2012. PMID: 22642194. DOI: 10.1007/978-3-0348-0364-9\_7
- 40 Spampinato SF, Merlo S, Sano Y, Kanda T and Sortino MA: Astrocytes contribute to A $\beta$ -induced blood-brain barrier damage through activation of endothelial MMP9. *J Neurochem* 142: 464-477, 2017. PMID: 28488764. DOI: 10.1111/jnc.14068
- 41 Vempati P, Popel AS and Mac Gabhann F: Extracellular regulation of VEGF: Isoforms, proteolysis, and vascular patterning. *Cytokine Growth Factor Rev* 25: 1-19, 2014. PMID: 24332926. DOI: 10.1016/j.cytogfr.2013.11.002
- 42 Jadhav U, Chigurupati S, Lakka SS and Mohanam S: Inhibition of matrix metalloproteinase-9 reduces *in vitro* invasion and angiogenesis in human microvascular endothelial cells. *Int J Oncol* 25: 1407-1414, 2004. PMID: 15492832. DOI: 10.3892/ijo.25.5.1407
- 43 Annabi B, Lachambre MP, Plouffe K, Moumdjian R and Béliveau R: Propranolol adrenergic blockade inhibits human brain endothelial cells tubulogenesis and matrix metalloproteinase-9 secretion. *Pharmacol Res* 60: 438-445, 2009. PMID: 19467330. DOI: 10.1016/j.phrs.2009.05.005
- 44 Lou M, Wang W, Yin J, Chen X, Cui D and Gu S: Aberrant activation of Hedgehog/Gli1 pathway on angiogenesis in gliomas. *Neurol India* 60: 589-596, 2012. PMID: 23287320. DOI: 10.4103/0028-3886.105192
- 45 Lee Y, Lee JK, Ahn SH, Lee J and Nam DH: WNT signaling in glioblastoma and therapeutic opportunities. *Lab Invest* 96: 137-150, 2016. PMID: 26641068. DOI: 10.1038/labinvest.2015.140
- 46 Gagliardi F, Narayanan A, Reni M, Franzin A, Mazza E, Boari N, Bailo M, Zordan P and Mortini P: The role of CXCR4 in highly malignant human gliomas biology: Current knowledge and future directions. *Glia* 62: 1015-1023, 2014. PMID: 24715652. DOI: 10.1002/glia.22669
- 47 Piaseczny MM, Pio GM, Chu JE, Xia Y, Nguyen K, Goodale D and Allan A: Generation of organ-conditioned media and applications for studying organ-specific influences on breast cancer metastatic behavior. *J Vis Exp* 112: 54037, 2016. PMID: 27341354. DOI: 10.3791/54037
- 48 Faria J, Romão L, Martins S, Alves T, Mendes FA, De Faria GP, Hollanda R, Takiya C, Chimelli L, Morandi V, De Souza JM, Abreu JG and Neto VM: Interactive properties of human glioblastoma cells with brain neurons in culture and neuronal modulation of glial laminin organization. *Differentiation* 74: 562-572, 2006. PMID: 17177853. DOI: 10.1111/j.1432-0436.2006.00090.x
- 49 Solito R, Corti F, Fossati S, Mezhericher E, Donnini S, Ghiso J, Giachetti A, Rostagno A and Ziche M: Dutch and arctic mutant peptides of  $\beta$  amyloid1-40 differentially affect the FGF-2 pathway in brain endothelium. *Exp Cell Res* 315: 385-395, 2009. PMID: 19061884. DOI: 10.1016/j.yexcr.2008.11.002
- 50 Towbin H, Staehelin T and Gordon J: Electrophoretic transfer of proteins from polyacrylamide gels to nitrocellulose sheets: procedure and some applications. *Proc Natl Acad Sci* 76: 4350-4354, 1979. PMID: 388439. DOI: 10.1073/pnas.76.9.4350
- 51 Yu JM, Jun ES, Jung JS, Suh SY, Han JY, Kim JY, Kim KW and Jung JS: Role of Wnt5a in the proliferation of human glioblastoma cells. *Cancer Lett* 257: 172-181, 2007. PMID: 17709179. DOI: 10.1016/j.canlet.2007.07.011
- 52 Kenig S, Alonso MBD, Mueller MM and Lah TT: Glioblastoma and endothelial cells cross-talk, mediated by SDF-1, enhances tumour invasion and endothelial proliferation by increasing expression of cathepsins B, S, and MMP-9. *Cancer Lett* 289: 53-61, 2010. PMID: 19700239. DOI: 10.1016/j.canlet.2009.07.014
- 53 Giusti I, Delle Monache S, Di Francesco M, Sanità P, D'Ascenzo S, Gravina GL, Festuccia C and Dolo V: From glioblastoma to endothelial cells through extracellular vesicles: messages for angiogenesis. *Tumor Biol* 37: 12743-12753, 2016. PMID: 27448307. DOI: 10.1007/s13277-016-5165-0
- 54 Pfaffl MW: A new mathematical model for relative quantification in real-time RT-PCR. *Nucleic Acids Res* 29: e45, 2001. PMID: 11328886. DOI: 10.1093/nar/29.9.e45
- 55 Albuquerque RJC, Hayashi T, Cho WG, Kleinman ME, Dridi S, Takeda A, Baffi JZ, Yamada K, Kaneko H, Green MG, Chappell J, Wilting J, Weich HA, Yamagami S, Amano S, Mizuki N, Alexander JS, Peterson ML, Brekken RA, Hirashima M, Capoor S, Usui T, Ambati BK and Ambati J: Alternatively spliced vascular endothelial growth factor receptor-2 is an essential endogenous inhibitor of lymphatic vessel growth. *Nat Med* 15: 1023-1030, 2009. PMID: 19668192. DOI: 10.1038/nm.2018
- 56 Charalambous C, Chen TC and Hofman FM: Characteristics of tumor-associated endothelial cells derived from glioblastoma multiforme. *Neurosurg Focus* 15: E22, 2006. PMID: 16709028. DOI: 10.3171/foc.2006.20.4.e22
- 57 Xu Y, Yuan FE, Chen QX and Liu BH: Molecular mechanisms involved in angiogenesis and potential target of antiangiogenesis in human glioblastomas. *Glioma* 1: 35-42, 2018. DOI: 10.4103/glioma.glioma\_10\_17
- 58 Korn C, Scholz B, Hu J, Srivastava K, Wojtarowicz J, Arnsperger T, Adams RH, Boutros M, Augustin HG and Augustin I: Endothelial cell-derived non-canonical Wnt ligands control vascular pruning in angiogenesis. *J Cell Sci* 141: 1757-1766, 2014. PMID: 24715464. DOI: 10.1242/dev.104422
- 59 Rao S, Sengupta R, Choe EJ, Woerner BM, Jackson E, Sun T, Leonard J, Pivnick-Worms D and Rubin JB: CXCL12 mediates trophic interactions between endothelial and tumor cells in glioblastoma. *PLoS One* 7: e33005, 2012. PMID: 22427929. DOI: 10.1371/journal.pone.0033005
- 60 Plate KH, Breier G, Weich HA, Mennel HD and Risau W: Vascular endothelial growth factor and glioma angiogenesis: Coordinate induction of VEGF receptors, distribution of VEGF protein and possible *In vivo* regulatory mechanisms. *Int J Cancer* 59: 520-529, 1994. PMID: 7525492. DOI: 10.1002/ijc.2910590415
- 61 Ladoux A and Frelin C: Expression of vascular endothelial growth factor by cultured endothelial cells from brain microvessels. *Biochem Biophys Res Commun* 194: 799-803, 1994. PMID: 8343163. DOI: 10.1006/bbrc.1993.1892
- 62 Lee TK, Poon RTP, Yuen AP, Ling MT, Wang XH, Wong YC, Guan XY, Man K, Tang ZY and Fan ST: Regulation of angiogenesis by Id-1 through hypoxia-inducible factor-1 $\alpha$ -mediated vascular endothelial growth factor up-regulation in hepatocellular carcinoma. *Clin Cancer Res* 12: 6910-6919, 2006. PMID: 17145808. DOI: 10.1158/1078-0432.CCR-06-0489

- 63 Vallée A, Guillevin R and Vallée JN: Vasculogenesis and angiogenesis initiation under normoxic conditions through Wnt/ $\beta$ -catenin pathway in gliomas. *Rev Neurosci* 29: 71-91, 2017. PMID: 28822229. DOI: 10.1515/revneuro-2017-0032
- 64 Pullen NA, Anand M, Cooper PS and Fillmore HL: Matrix metalloproteinase-1 expression enhances tumorigenicity as well as tumor-related angiogenesis and is inversely associated with TIMP-4 expression in a model of glioblastoma. *J Neurooncol* 106: 461-471, 2012. PMID: 21858729. DOI: 10.1007/s11060-011-0691-5
- 65 Thorgeirsson UP, Lindsay CK, Cottam DW and Gomez DE: Tumor invasion, proteolysis, and angiogenesis. *J Neurooncol* 18: 89-103, 1994. PMID: 7525888. DOI: 10.1007/bf01050415
- 66 Salmaggi A, Gelati M, Pollo B, Frigerio S, Eoli M, Silvani A, Broggi G, Ciusani E, Croci D, Boiardi A and De Rossi M: CXCL12 in malignant glial tumors: A possible role in angiogenesis and cross-talk between endothelial and tumoral cells. *J Neurooncol* 67: 305-317, 2004. PMID: 15164986. DOI: 10.1023/b:neon.0000024241.05346.24
- 67 Matias D, Dubois LG, Pontes B, Rosário L, Ferrer VP, Balça-Silva J, Fonseca ACC, Macharia LW, Romão L, e Spohr TCL de S, Chimelli L, Filho PN, Lopes MC, Abreu JG, Lima FRS and Moura-Neto V: GBM-derived Wnt3a induces M2-Like phenotype in microglial cells through Wnt/ $\beta$ -catenin signaling. *Mol Neurobiol* 56: 1517-1530, 2019. PMID: 29948952. DOI: 10.1007/s12035-018-1150-5
- 68 Garcia C, Dubois GG, Xavier LL, Geraldo HH, da Fonseca CCC, Correia HH, Meirelles F, Ventura G, Romão L, Canedo SHS, de Souza MM, de Menezes LRL, Moura-Neto V, Tovar-Moll F and Lima SRS: The orthotopic xenotransplant of human glioblastoma successfully recapitulates glioblastoma-microenvironment interactions in a non-immunosuppressed mouse model. *BMC Cancer* 14: 923, 2014. PMID: 25482099. DOI: 10.1186/1471-2407-14-923
- 69 Dowling P and Clynes M: Conditioned media from cell lines: A complementary model to clinical specimens for the discovery of disease-specific biomarkers. *Proteomics* 11: 794-804, 2011. PMID: 21229588. DOI: 10.1002/pmic.201000530
- 70 Bocci G: In-vitro evidence of autocrine secretion of vascular endothelial growth factor by endothelial cells from human placental blood vessels. *Mol Hum Reprod* 7: 771-777, 2001. PMID: 11470865. DOI: 10.1093/molehr/7.8.771
- 71 Bao Y, Liu B, Xiong Y, Shi J, Li P, Chen J, Zhang Z, Chen M, Wang L, Wu Z, Wang Z and Lu X: A feed-forward loop between nuclear translocation of CXCR4 and HIF-1 $\alpha$  promotes renal cell carcinoma metastasis. *Oncogene* 38: 881-895, 2018. PMID: 30177838. DOI: 10.1038/s41388-018-0452-4
- 72 Ngo MT and Harley BA: The influence of hyaluronic acid and glioblastoma cell coculture on the formation of endothelial cell networks in gelatin hydrogels. *Adv Healthc Mater* 6(22), 2017. PMID: 28941173. DOI: 10.1002/adhm.201700687
- 73 Kargiotis O, Rao JS and Kyritsis AP: Mechanisms of angiogenesis in gliomas. *J Neurooncol* 78: 281-293, 2006. PMID: 16554966. DOI: 10.1007/s11060-005-9097-6
- 74 Liu Y, Beyer A and Aebersold R: On the dependency of cellular protein levels on mRNA abundance. *Cell* 165: 535-550, 2016. PMID: 27104977. DOI: 10.1016/j.cell.2016.03.014
- 75 Tang M, Yang Y, Yu J, Wu N, Chen P, Xu L, Wang Q, Xu Z, Ge J, Yu K and Zhuang J: Discordant mRNA and protein expression of CXCR4 under *in vitro* CoCl<sub>2</sub>-induced hypoxic conditions. *Biochem Biophys Res Commun* 484: 285-291, 2017. PMID: 28126341. DOI: 10.1016/j.bbrc.2017.01.102
- 76 Breier G, Albrecht U, Sterrer S and Risau W: Expression of vascular endothelial growth factor during embryonic angiogenesis and endothelial cell differentiation. *Development* 114: 521-532, 1992. PMID: 1592003.
- 77 Tsai J-C, Goldman CK and Gillespie GY: Vascular endothelial growth factor in human glioma cell lines: induced secretion by EGF, PDGF-BB, and bFGF. *J Neurosurg* 82: 864-873, 2009. PMID: 7714613. DOI: 10.3171/jns.1995.82.5.0864
- 78 Hoeben A, Landuyt B, Highley MS, Wildiers H, Van Oosterom AT and De Bruijn EA: Vascular endothelial growth factor and angiogenesis. *Pharmacol Rev* 56: 549-580, 2004. PMID: 15602010. DOI: 10.1124/pr.56.4.3
- 79 Nag S: Morphology and properties of brain endothelial cells. *Methods Mol Biol* 686: 3-47, 2010. PMID: 21082365. DOI: 10.1007/978-1-60761-938-3\_1
- 80 Domigan CK, Warren CM, Antanesian V, Happel K, Ziyad S, Lee S, Krall A, Duan L, Torres-Collado AX, Castellani LW, Elashoff D, Christofk HR, van der Bliek AM, Potente M and Iruela-Arispe ML: Autocrine VEGF maintains endothelial survival through regulation of metabolism and autophagy. *J Cell Sci* 128: 2236-2248, 2015. PMID: 25956888. DOI: 10.1242/jcs.163774
- 81 Napione L, Pavan S, Veglio A, Picco A, Boffetta G, Celani A, Seano G, Primo L, Gamba A and Bussolino F: Unraveling the influence of endothelial cell density on VEGF-A signaling. *Blood* 119: 5599-5607, 2012. PMID: 22510875. DOI: 10.1182/blood-2011-11-390666
- 82 Holmes K, Roberts OL, Thomas AM and Cross MJ: Vascular endothelial growth factor receptor-2: Structure, function, intracellular signalling and therapeutic inhibition. *Cell Signal* 19: 2003-2017, 2007. PMID: 17658244. DOI: 10.1016/j.cellsig.2007.05.013
- 83 Kumar S and Arbab AS: Neovascularization in glioblastoma: Current pitfall in anti-angiogenic therapy. *Zhong Liu Za Zhi* 1: 16-19, 2013. PMID: 24976869.
- 84 Lu KV and Bergers G: Mechanisms of evasive resistance to anti-VEGF therapy in glioblastoma. *CNS Oncol* 2: 49-65, 2013. PMID: 23750318. DOI: 10.2217/cns.12.36
- 85 Fitzgerald G, Soro-Arnaiz I and De Bock K: The Warburg effect in endothelial cells and its potential as an anti-angiogenic target in cancer. *Front Cell Dev Biol* 6: 100, 2018. PMID: 30255018. DOI: 10.3389/fcell.2018.00100

Received March 18, 2020

Revised March 30, 2020

Accepted March 31, 2020